

Unusual hysteresis and giant low-field magnetoresistance in polycrystalline sample with nominal composition of $\text{La}_{2/3}\text{Ca}_{1/3}\text{Mn}_{0.955}\text{Cu}_{0.045}\text{O}_3$

S. L. Yuan, Y. P. Yang, Z. C. Xia, L. Liu, G. H. Zhang, W. Feng, J. Tang, L. J. Zhang, and S. Liu
Department of Physics, Huazhong University of Science and Technology, Wuhan 430074, People's Republic of China
 (Received 3 September 2002; published 7 November 2002)

Unusual thermal and magnetic hysteresis is observed near the insulator-metal transition of $\text{La}_{2/3}\text{Ca}_{1/3}\text{Mn}_{1-x}\text{Cu}_x\text{O}_3$ ($x=4.5\%$). For the temperature range at which the hysteresis appears, the sample shows unusual giant magnetoresistance (MR) behavior even for a low field of ~ 0.3 T. The maximum MR has a value of $\Delta\rho/\rho(H=0)$ as high as $\sim 90\%$ for the 0.3 T field. A possible discussion is presented by considering the sample as a granular system consisting of manganese grains surrounded by some surface layer created due to the Cu segregation towards the grain surface.

DOI: 10.1103/PhysRevB.66.172402

PACS number(s): 75.30.Vn, 72.15.Gd, 74.72.Dn

The discovery of colossal magnetoresistance (CMR) in mixed-valence manganites of the type $\text{La}_{1-x}\text{Ca}_x\text{MnO}_3$ has motivated the wide research on these compounds.^{1,2} A rich phase diagram³ has been revealed as a function of temperature and doping content that is due to the intricate interplay of charge, spin, orbital, and lattice degrees of freedom.⁴ In view of the competing character of these interactions, varying x can greatly affect their intrinsic properties including paramagnetic-ferromagnetic (PM-FM) transitions at T_C and CMR. For $x \sim 1/3$, the CMR shows a peak near T_C and substantially decreases on varying the temperature from T_C . Much exploration has been done through doping of La sites with other smaller ions,⁵ which brings strong lattice effects on these interactions. An interesting way is to dope at the Mn sites of $\text{La}_{2/3}\text{Ca}_{1/3}\text{MnO}_3$ by other transition elements,⁶⁻¹⁰ which can modify the $\text{Mn}^{3+}\text{-O-Mn}^{4+}$ network and in turn largely affects their intrinsic properties. In most cases, a low-level doping can cause an obvious shift of PM-FM transition to lower temperatures and a substantial enhancement in CMR. It, however, is found on a magnetic field scale of several teslas, which is not very appealing for applications.

Much effort has been made to understand the physical properties of manganites, which led to the discovery of another type of MR, namely, intergrain MR in polycrystalline manganites.¹¹⁻¹⁶ Intergrain MR can be observed at low fields but has larger values only at $T \ll T_C$. Although the CMR near T_C is an intrinsic property of manganites, extrinsic influences (such as grain size in polycrystalline samples) dramatically modify this response. This could lead to a complex behavior in which both effects (intrinsic CMR and extrinsic intergrain MR) are present at the same time.¹⁵ Here we report investigations of the transport and magnetic properties of $\text{La}_{2/3}\text{Ca}_{1/3}\text{Mn}_{1-x}\text{Cu}_x\text{O}_3$ polycrystalline samples ($x=0$ and 4.5%) synthesized by a sol-gel method. It is interesting to find that for the temperature range at which the remarkable thermal and magnetic hysteresis is revealed, the $x=4.5\%$ sample shows unusual MR behavior under low applied magnetic fields. The maximum MR observed near the insulator-metal (I - M) transition reaches a value of $\Delta\rho/\rho(H=0) \sim 90\%$ for a field as low as ~ 0.3 T.

A sol-gel method was used to prepare polycrystalline samples of nominal composition $\text{La}_{2/3}\text{Ca}_{1/3}\text{Mn}_{1-x}\text{Cu}_x\text{O}_3$ (x

$=0$ and 4.5%). This method includes two main steps. One is the preparation of nanometric powders similar to a previous description.¹³ Another is the formation of perovskite structure by a sintering treatment at the temperature T_s for the sol-gel prepared powders. One advantage of this method lies in a wide range for T_s to obtain a single-phase sample with perovskite structure. The T_s is shown to be a key factor to control the average grain size;^{13,15} usually, the smaller grain size is obtained in the case of lower T_s . For the present samples, the sol-gel prepared powders were ground, pelletized, and then sintered at $T_s = 1100^\circ\text{C}$ for 12 h. From previous studies,^{13,15} the average grain size of the samples prepared at $T_s = 1100^\circ\text{C}$ is estimated to be the order of ~ 100 nm. The structural characterization was done through x-ray diffraction at room temperature. Results indicate that the same diffraction pattern is obtained in both the $x=0$ and 4.5% samples, and all the observed diffraction peaks can be indexed into a perovskite crystalline structure. Within the accuracy of the measurement, no evidence is found for the presence of any Cu-dependent secondary phase.

Transport and magnetic properties were measured in a commercial Physical Property Measurement System (Quantum Design PPMS). Indicated by solid circles in Fig. 1 is the resistivity (ρ) versus temperature (T) curve measured in the $x=0$ sample for zero magnetic field during cooling. The

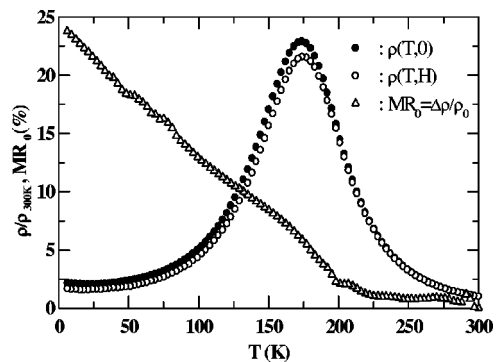


FIG. 1. Temperature dependence of normalized resistivity for zero (solid circles) and an applied field of 0.3 T (open circles) as well as the corresponding magnetoresistance (open triangles) for $\text{La}_{2/3}\text{Ca}_{1/3}\text{MnO}_3$.

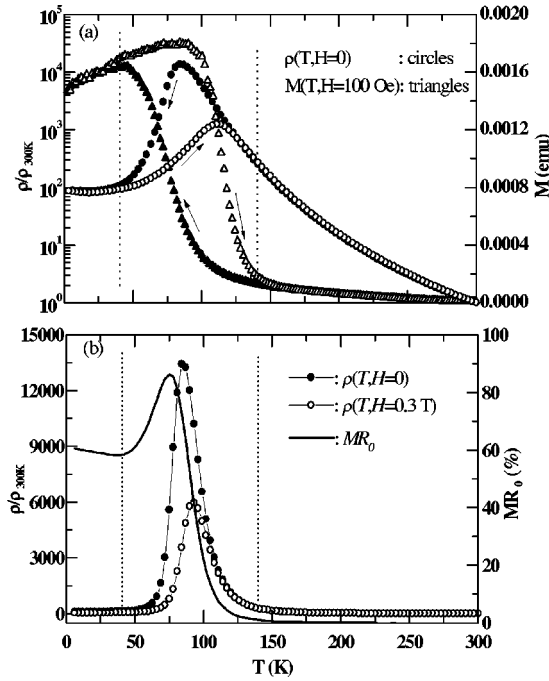


FIG. 2. Temperature dependence of (a) normalized resistivity in zero field and dc magnetization measured in 100 Oe, where arrows indicate the temperature running direction, and (b) normalized resistivity measured for fields of $H=0$ and 0.3 T as well as the corresponding magnetoresistance for the $x=4.5\%$ sample.

sample shows an insulating behavior at high temperatures and metallic behavior at low temperatures. The I - M transition characterized by a peak occurs at $T_{MI} \sim 175$ K, a much lower value as compared with the corresponding ceramic sample, which can be attributable to the increased grain boundary (GB) effect caused by smaller grain size due to lower T_s . The zero-field ρ - T curve during warming was also measured (not shown), and no difference is found for both the modes, indicating no thermal hysteresis in this sample. When a low field is applied, as indicated by open circles in Fig. 1 for a field of $H=0.3$ T, the sample shows a small reduction in ρ at low temperatures. Defining the MR as

$$MR_0(\%) = \frac{\rho(T, H=0) - \rho(T, H)}{\rho(T, H=0)} \times 100\%, \quad (1)$$

we obtain MR_0 as a function of temperature for the 0.3 T field as indicated by triangle symbols in Fig. 1. It can be seen that the $x=0$ sample shows typical features of intergrain MR in which MR_0 monotonically increases on cooling.

This picture changes when Cu is introduced into the system. The zero-field ρ - T curves for the $x=4.5\%$ sample are displayed by solid and open circles in Fig. 2(a) for both the cooling and warming-up modes, respectively. Three distinguishable regions can be found in this measurement: (1) high temperature of $T > \sim 140$ K (region I), (2) middle temperature of $\sim 40 \text{ K} < T < \sim 140$ K (region II), and (3) low temperature of $T < \sim 40$ K (region III). At regions I and III, no thermal hysteresis is revealed, where both the $\rho(T, H=0)$ curves obtained in the cooling and warming-up modes are

exactly the same. At region II, $\rho(T, H=0)$ reveals a large thermal hysteresis in the cooling and warming-up modes. It is also noted that $\rho(T, H=0)$ data obtained in the cooling mode are larger than that in the warming-up mode and the thermal hysteresis becomes the most remarkable near the temperature ~ 75 K below which the sample undergoes a transition to a metallic state on cooling.

Indicated by open and solid triangles in Fig. 2(a) are zero-field-cooled (ZFC) and field-cooled (FC) magnetization data, respectively, measured in the $x=4.5\%$ sample for a field of 100 Oe. One can note that the three regions revealed in the measurement of $\rho(T, H=0)$ are also present in the magnetic measurement. Both the FC and ZFC data coincide at regions I and III, but a large deviation between FC and ZFC data appears at region II where the ZFC data are larger than the FC data. This observation is obviously different from that commonly observed in spin glasses. For spin glasses, the deviation between FC and ZFC data appears at low temperatures and the FC data are larger than the ZFC data. It is therefore suggested that any consideration based on the spin frustration is inappropriate for the present observation of magnetic hysteresis.

In Fig. 2(b) we plot the ρ - T curve measured during cooling for the 0.3 T field (open circles) together with the corresponding zero-field curve (solid circles) for the $x=4.5\%$ sample. It can be readily noted that applying such a low field causes a substantial decrease in the peak resistivity and a clear shift of the I - M transition to higher temperature. Using Eq. (1), MR_0 is calculated as a function of temperature, which is displayed by the solid line in Fig. 2(b). It is obvious that different behaviors are revealed at different temperature regions. At region I, no sizable MR effect is found, while at region III, the sample shows characteristic features of intergrain MR which shows a monotonic increase on cooling towards 0 K. Compared to the $x=0$ sample, the $x=4.5\%$ sample shows a substantial enhancement in the intergrain MR. The largest value appearing at $T \rightarrow 0$ increases from $\sim 25\%$ to $\sim 60\%$ with x from 0 to 4.5%. Much to our surprise is the MR observed at region II. It is characterized by a peak appearing near the I - M transition temperature (~ 75 K) with a value as high as $\sim 90\%$. As temperature is decreased or increased from ~ 75 K, the MR shows a substantial reduction from its maximum value. This is a characteristic feature for the observation of CMR. For manganites showing CMR, however, this characteristic feature is found only on a magnetic field scale of several teslas. For the present sample, this characteristic feature is seen even for a field as low as 0.3 T.

An essential fact should be noted in Fig. 2; namely, an unusually large MR effect is observed at the temperature region where the (thermal and magnetic) hysteresis becomes the most remarkable, suggesting the same underlying physical origin for them. In order to gain some information for this understanding, here we perform measurements of the MR dependence on magnetic field. Three typical temperatures of $T=140$, 75, and 4 K are selected for this study. Before each measurement, the sample was always heated to room temperature and then cooled to the desired temperature in zero field. Keeping this temperature, the measurement was

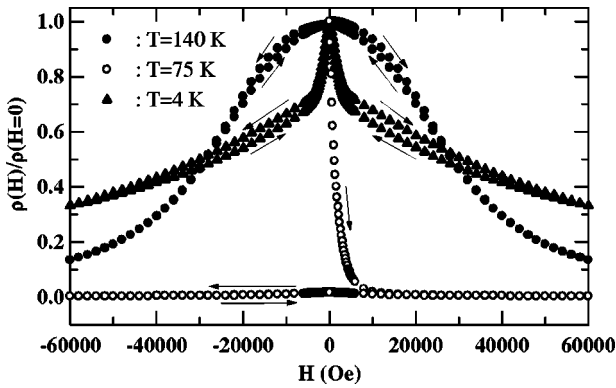


FIG. 3. Field dependence of resistivity at $T=140$, 75 , and 4 K for the $x=4.5\%$ sample. Arrows indicate the field sweeping direction.

carried out by sweeping the magnetic field according to $0 \rightarrow H_{\max} \rightarrow 0 \rightarrow -H_{\max} \rightarrow 0$. Shown in Fig. 3 are the thus obtained ρ - H curves. At $T=140$ K, a temperature above which the hysteresis disappears, the field dependence (solid circles in Fig. 3) is basically reversible and the MR becomes observable only when higher fields ($> \sim 1$ T) are applied. At 6 T, MR_0 reaches a value $\sim 87\%$. This behavior in MR is similar to that commonly observed in manganites and the field-induced alignment of Mn spins should be responsible for the observed MR. At $T=4$ K which is located at region III, as demonstrated by solid triangles in Fig. 3, the application of fields first causes a sharp decrease in ρ and then a more gradual decrease on further increasing field. The sharp decrease in ρ at low fields originates from the field-induced rotation of FM domains. A small amount of hysteresis is present that is due to the interplay of domains. These observations indicate that the present sample at low temperatures shows typical features of grain ferromagnets.

As indicated by open circles in Fig. 3, the $x=4.5\%$ sample at region II shows very peculiar behavior. Before sweeping the field, the sample is of a “high- ρ ” state with $\rho(H)/\rho(H=0) \sim 1$. On sweeping the field, the sample quickly enters into a “low- ρ ” state with $\rho(H)/\rho(H=0) \sim 0$. With sweeping H up to ~ 0.7 T or above, the sample shows a weak field dependence. After sweeping the field to 6 T and then back to zero again, the sample does not return its previous “high- ρ ” state but maintains its “low- ρ ” level. The difference between two curves measured on sweeping H from 0 to the maximum and then back to 0 from the maximum therefore is a measure of the “remanence” of the MR, indicating that the sample “remembers” the maximum value of the magnetic field which had been applied. Once this “low- ρ ” state is created, it is metastable and persists after the removal of the applied field. After the first run for the field sweeping, the sample maintains this “low- ρ ” state and no magnetic hysteresis is observed on sweeping the field from 0 to $-H_{\max}$ and then from $-H_{\max}$ to H_{\max} and last back to 0. This “low- ρ ” state is destroyed and the sample is returned to its previous behavior only when the sample is heated to high temperatures (> 140 K).

The results indicated in Fig. 2 clearly demonstrate the same underlying physical origin for unusual MR and hysteresis

phenomena observed near the I - M transition. Because of the absence of these unusual phenomena in the $x=0$ sample, it is therefore natural to attribute them to be caused by the introduction of Cu into the system. As is well known, the $\text{Cu}^{2+}(d^9)$ ion has a larger ionic radius as compared to the average Mn radius; it is therefore likely that Cu ions in the proximity of the GB are attracted towards the boundary in order to release the local strain.⁷ This is expected to occur more easily as the grain size becomes small. This leads to the possibility that the sample is a granular one consisting of manganese perovskite grains surrounded by surface layers created by some Cu-dependent material.

At present, we cannot identify the exact nature of the GB created by some Cu-dependent material. However, we believe that its presence would be responsible for those unusual observations. Since Cu itself is a PM ion, it is likely that Cu spins present at the GB perhaps plays a role as the medium of FM coupling between neighboring FM grains. Plotting H/M as a function of temperature, where M is the FC data indicated by solid triangles in Fig. 2(a), one would find two distinct magnetic transition temperatures $T_{C1} \sim 230$ K and $T_{C2} \sim 75$ K. The thus estimated T_{C1} is almost the same as T_C of the $x=0$ sample. This is indicative of the alignment of Mn spins within grains below T_{C1} for the $x=4.5\%$ sample. Although the Mn spins are ferromagnetically aligned within grains, the magnetic moments between FM grains are not parallel due to the spin disordering at the GB. As a result, insulating behavior is maintained to temperatures much lower than T_{C1} . On cooling from T_{C1} , the spins at the GB tend to align along one of the FM grains. This in turn would affect the alignment of the magnetic moment from its neighboring FM grains. As a result, the magnetic moments between neighboring FM grains tend to align along the same direction on cooling to a temperature T_{C2} , causing a transition to metallic state below this temperature. Once the spins at the GB are aligned in such a way, the sample “remembers” their alignment. Because of this remembrance, ZFC magnetization data should be larger than FC data, while the $\rho(T, H=0)$ measured in the warming-up mode should be smaller than that in the cooling mode, for the temperature range located at region II. Only when the sample is heated to temperatures higher than ~ 140 K does the remembrance disappear and then the (thermal and magnetic) hysteresis vanish.

A similar discussion can be done for the $\rho(T, H)$ measured at $T=75$ K. At zero field, the ρ is high due to the spin disordering at the GB. Upon application of magnetic fields, the spins at the GB tend to align along the field direction, which in turn further affects the alignment of neighboring FM grains. As a result, the ρ shows a sharp decrease. When a high enough field ($> \sim 0.7$ T) is applied, the spins at the GB and magnetic moments from FM grains are aligned almost along the same direction. In this situation, the ρ is low and shows a weak field dependence. After the first run for the field sweeping, the sample “remembers” the previous alignment for the spins at the GB. Therefore, the sample maintains its “low- ρ ” state and no magnetic hysteresis is ob-

served on sweeping the field from 0 to $-H_{\max}$ and then from $-H_{\max}$ to H_{\max} and last back to 0.

Once the above interpretation is accepted, the observed low-field MR at region II can be explained quite naturally. The application of fields decreases the random distribution of the spins at the GB, leading to a large decrease in ρ and hence the sizable MR. For the well-known manganites, the CMR is due to the field-induced alignment of Mn spins. Therefore, comparably high fields of several teslas are required to obtain a sizable effect. For the present situation, application of the fields aligns the spins at the GB, which in turn align the magnetic moments of neighboring grains which have been ferromagnetically ordered at higher temperatures. Therefore, it is likely that a sizable MR can be realized even in low fields.

In summary, we have shown that the MR with a value of $\Delta\rho/\rho(H=0)\sim 90\%$ for the 0.3 T field can be realized upon 4.5% Cu being introduced into $\text{La}_{2/3}\text{Ca}_{1/3}\text{MnO}_3$. Such a low-field giant MR is found to appear at the temperature range at which the sample shows remarkable thermal and magnetic hysteresis effects. Our results also point to the physical origin of the observed low-field giant MR different from the CMR commonly observed near the PM-FM transition for manganese perovskites.

The authors thank Dr. Tovstolytkin (Ukraine) for useful discussions. This work was supported by the National Science Foundation of China (Grant No. 10174022) and Trans-Century Training Program Foundation for the Talents by the Ministry of Education.

¹R. von Helmolt *et al.*, Phys. Rev. Lett. **71**, 2331 (1993).

²S. Jin, T.H. Tiefel, M. McCormack, R.A. Fastnacht, R. Ramesh, and L.H. Chen, Science **264**, 413 (1994).

³P. Schiffer, A.P. Ramirez, W. Bao, and S.-W. Cheong, Phys. Rev. Lett. **75**, 3336 (1995).

⁴A. Moreo, S. Yunoki, and E. Dagotto, Science **283**, 2034 (1999).

⁵H.Y. Hwang, S.-W. Cheong, P.G. Radaelli, M. Marezio, and B. Batlogg, Phys. Rev. Lett. **75**, 914 (1995).

⁶R. von Helmolt, L. Haupt, K. Barner, and U. Sondermann, Solid State Commun. **82**, 693 (1992).

⁷K. Ghosh, S.B. Ogale, R. Ramesh, R.L. Greene, T. Venkatesan, K.M. Gapchup, R. Bathe, and S.I. Patil, Phys. Rev. B **59**, 533 (1999).

⁸S.A. Sergeenkov, H. Bourgrine, M. Ausloos, and R. Cloots, JETP Lett. **69**, 858 (1999).

⁹S.L. Yuan *et al.*, Eur. Phys. J. B **20**, 177 (2001); Solid State Com-

mun. **117**, 661 (2001).

¹⁰A.I. Tovstolytkin, A.N. Pogorily, E.V. Shypil, and D.I. Podyalovski, Phys. Met. Metallogr. **91**, S214 (2001).

¹¹H.Y. Hwang, S.-W. Cheong, N.P. Ong, and B. Batlogg, Phys. Rev. Lett. **77**, 2041 (1996).

¹²A. Gupta, G.Q. Gong, G. Xiao, P.R. Duncombe, P. Lecoeur, P. Trouilloud, Y.Y. Wang, V.P. Dravid, and J.Z. Sun, Phys. Rev. B **54**, R15 629 (1996).

¹³R.D. Sanchez, J. Rivas, C. Vazquez, M.A. Lopez-Quintela, M.T. Causa, M. Tovar, and S. Oseroff, Appl. Phys. Lett. **68**, 134 (1996).

¹⁴R. Mahesh, R. Mahendiran, A.K. Raychaudhuri, and C.N.R. Rao, Appl. Phys. Lett. **68**, 2291 (1996).

¹⁵L.E. Hueso, J. Rivas, F. Rivadula, and M.A. Lopez-Quintela, J. Appl. Phys. **86**, 3881 (1999).

¹⁶M. Ziese, Rep. Prog. Phys. **65**, 143 (2002).